

Preparation, Reactivity, and Structural Peculiarities of Hydroxyalkyl-Functionalized “Second-Generation” Ruthenium Carbene Complexes

Stefan Prühs, Christian W. Lehmann, and Alois Fürstner*

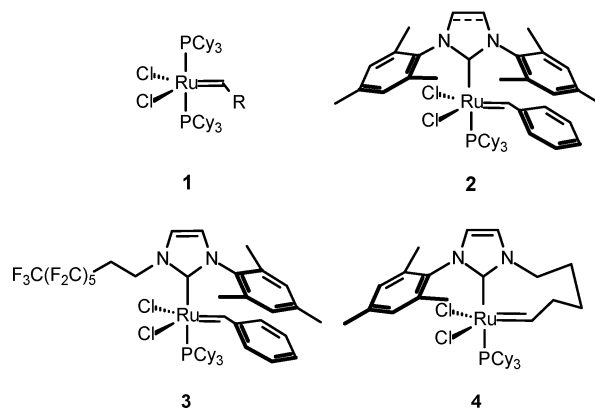
Max-Planck-Institut für Kohlenforschung, D-45470 Mülheim/Ruhr, Germany

Received September 26, 2003

The preparation, immobilization, and structure of “second-generation” ruthenium benzyldiene metathesis catalysts bearing hydroxyalkyl chains on their N-heterocyclic carbene ligands are described. Complexes of this type are prone to rearrange their ligand sphere such that the neutral ligands get *cis*- rather than *trans*-disposed. Moreover, treatment of complex **7d** with pyridine results in an unprecedented ionization by loss of one of its chloride ligands. The resulting cationic species **13**, though devoid of catalytic activity, is the first member of a new type of ruthenium carbene complexes characterized by an octahedral coordination geometry and a donor/acceptor interaction between the metal center and the tethered hydroxyl group. The *trans*-configured hydroxyalkyl-functionalized complexes **8a** and **8b**, the *cis*-configured compound **10**, and the ion pair **13** have been structurally characterized by X-ray crystallography.

The advent of ruthenium carbene complexes of the general type **1**¹ and “second-generation” variants **2** bearing N-heterocyclic carbene (NHC) ligands^{2,3} has revolutionized alkene metathesis during the past decade. These catalysts combine high efficiency with a previously unknown functional group tolerance and are exceedingly practical tools for organic synthesis and polymer chemistry.^{4,5} Although some applications to commercial products have already followed,⁶ it is expected that their impact on fine chemical production will further increase to the extent to which the total attain-

able turnover number rises, the necessary catalyst loading can be reduced, metal impurities in the resulting products can be minimized, and/or the physical properties of the catalysts can be adjusted to the specific requirements of a given production process.



* To whom correspondence should be addressed. E-mail: fuerstner@mpi-muelheim.mpg.de. Fax: +49 208 306 2994. Tel: +49 208 306 2342.

(1) (a) Nguyen, S. T.; Grubbs, R. H.; Ziller, J. W. *J. Am. Chem. Soc.* **1993**, *115*, 9858. (b) Schwab, P.; Grubbs, R. H.; Ziller, J. W. *J. Am. Chem. Soc.* **1996**, *118*, 100.

(2) (a) Huang, J.; Stevens, E. D.; Nolan, S. P.; Petersen, J. L. *J. Am. Chem. Soc.* **1999**, *121*, 2674. (b) Scholl, M.; Trnka, T. M.; Morgan, J. P.; Grubbs, R. H. *Tetrahedron Lett.* **1999**, *40*, 2247. (c) Ackermann, L.; Fürstner, A.; Weskamp, T.; Kohl, F. J.; Herrmann, W. A. *Tetrahedron Lett.* **1999**, *40*, 4787. (d) Weskamp, T.; Kohl, F. J.; Hieringer, W.; Gleich, D.; Herrmann, W. A. *Angew. Chem.* **1999**, *111*, 2573; *Angew. Chem., Int. Ed.* **1999**, *38*, 2416. (e) Scholl, M.; Ding, S.; Lee, C. W.; Grubbs, R. H. *Org. Lett.* **1999**, *1*, 953. (f) Fürstner, A.; Thiel, O. R.; Ackermann, L.; Schanz, H.-J.; Nolan, S. P. *J. Org. Chem.* **2000**, *65*, 2204.

(3) For further important variants see i.a.: (a) Kingsbury, J. S.; Harrity, J. P. A.; Bonitatebus, P. J., Jr.; Hoveyda, A. H. *J. Am. Chem. Soc.* **1999**, *121*, 791. (b) Gessler, S.; Randl, S.; Blechert, S. *Tetrahedron Lett.* **2000**, *41*, 9973. (c) Fürstner, A.; Guth, O.; Duffels, A.; Seidel, G.; Liebl, M.; Gabor, B.; Mynott, R. *Chem. Eur. J.* **2001**, *7*, 4811. (d) Fürstner, A.; Liebl, M.; Lehmann, C. W.; Picquet, M.; Kunz, R.; Bruneau, C.; Touchard, D.; Dixneuf, P. H. *Chem. Eur. J.* **2000**, *6*, 1847.

(4) (a) *Handbook of Metathesis, Vol. I–III*; Grubbs, R. H., Ed.; Wiley-VCH: Weinheim, 2003. (b) *Alkene Metathesis in Organic Synthesis*; Fürstner, A., Ed.; Springer: Berlin, 1998.

(5) General reviews: (a) Trnka, T. M.; Grubbs, R. H. *Acc. Chem. Res.* **2001**, *34*, 18. (b) Fürstner, A. *Angew. Chem.* **2000**, *112*, 3140; *Angew. Chem., Int. Ed.* **2000**, *39*, 3012. (c) Grubbs, R. H.; Chang, S. *Tetrahedron* **1998**, *54*, 4413. (d) Fürstner, A. *Top. Catal.* **1997**, *4*, 285. (e) Connon, S. J.; Blechert, S. *Angew. Chem.* **2003**, *115*, 1944; *Angew. Chem., Int. Ed.* **2003**, *42*, 1900. (f) Schrock, R. R. *Top. Organomet. Chem.* **1998**, *1*, 1.

(6) Pederson, R. L.; Fellows, I. M.; Ung, T. A.; Ishihara, H.; Hajela, S. P. *Adv. Synth. Catal.* **2002**, *344*, 728.

In an attempt to develop such “designer” catalysts with tailor-made properties we have previously shown that substantial structural variations can be accommodated at the NHC ligand without compromising the catalytic efficiency.⁷ On this basis, it was possible to develop catalysts for applications in fluorous media or supercritical CO₂ (e.g., **3**)⁸ and to prepare chelate complexes such as **4** that are able to regenerate themselves once productive metathesis has ceased;⁷ the latter also turned out to be instrumental for the synthesis of

(7) (a) Fürstner, A.; Ackermann, L.; Gabor, B.; Goddard, R.; Lehmann, C. W.; Mynott, R.; Stelzer, F.; Thiel, O. R. *Chem. Eur. J.* **2001**, *7*, 3236. (b) Fürstner, A.; Krause, H.; Ackermann, L.; Lehmann, C. W. *Chem. Commun.* **2001**, 2240.

(8) (a) Fürstner, A.; Ackermann, L.; Beck, K.; Hori, H.; Koch, D.; Langemann, K.; Liebl, M.; Six, C.; Leitner, W. *J. Am. Chem. Soc.* **2001**, *123*, 9000. (b) Fürstner, A.; Koch, D.; Langemann, K.; Leitner, W.; Six, C. *Angew. Chem.* **1997**, *109*, 2562; *Angew. Chem., Int. Ed. Engl.* **1997**, *36*, 2466.

previously inaccessible speciality polymers.⁹ In pursuit of this concept, we became interested in ruthenium-carbene complexes bearing hydroxyalkyl groups on their NHC ligands which might lend themselves for immobilization on various supports.^{10–12} During these investigations, however, an unknown bias of such systems for rearrangement of their ligand sphere was observed that sheds light on the as yet not fully explored fluxional behavior of ruthenium complexes of this type.

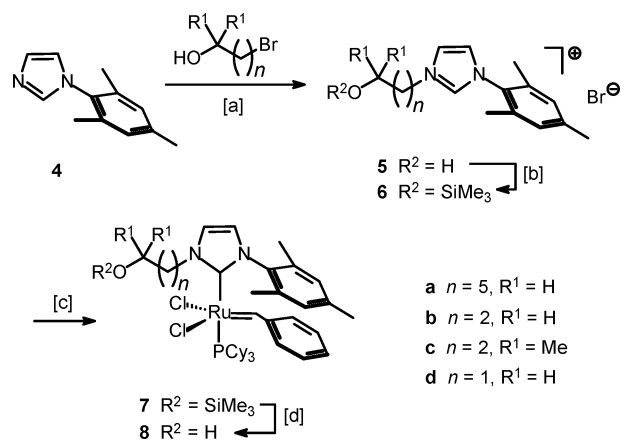
The preparation of these species is straightforward and essentially follows the established routes (Scheme 1). Thus, reaction of *N*-mesitylimidazole **4** with commercially available 1-hydroxy-*ω*-bromoalkanes affords the corresponding imidazolium salts **5a–d** which are O-silylated on treatment with hexamethyldisilazane and catalytic amounts of TMSCl in refluxing CH₂Cl₂. This reagent combination is particularly convenient, as the workup consists only of the evaporation of all volatile components without need to remove byproducts from the resulting imidazolium salts **6a–d**. Their deprotonation with KOTBu in toluene in the presence of complex **1** (R = Ph)¹ at ambient temperature affords the desired functionalized NHC complexes **7a–d**, although the isolated yields are only moderate. The subsequent desilylation step, in contrast, is invariably high yielding when carried out with catalytic amounts of HCl in CH₂Cl₂/MeOH, affording the targeted ruthenium-NHC complexes **8a–c** bearing *unprotected* hydroxyl groups in their side chains (for **8d**, see below). All spectroscopic and analytical data of these dark red compounds, which are moderately stable in solution, are in accordance with the proposed structures that have been confirmed by

(9) (a) Bielawski, C. W.; Benitez, D.; Grubbs, R. H. *Science* **2002**, *297*, 2041. (b) Bielawski, C. W.; Benitez, D.; Grubbs, R. H. *J. Am. Chem. Soc.* **2003**, *125*, 8424.

(10) The immobilization of ruthenium carbene complexes has previously been carried out mainly via the (hemi)labile ligands in an attempt to combine the advantages of homogeneous and heterogeneous catalysis into a single manifold ("release-capture" or "boomerang" mechanism), cf. ref 11. Only a few examples of ruthenium carbene complexes immobilized through the kinetically more inert NHC- or the anionic ligands have been reported in the literature, cf.: (a) Schürer, S. C.; Gessler, S.; Buschmann, N.; Blechert, S. *Angew. Chem.* **2000**, *112*, 4062; *Angew. Chem., Int. Ed.* **2000**, *39*, 3898. (b) Mayr, M.; Mayr, B.; Buchmeiser, M. R. *Angew. Chem.* **2001**, *113*, 3957; *Angew. Chem., Int. Ed.* **2001**, *40*, 3839. (c) Krause, J. O.; Lubbad, S.; Nuyken, O.; Buchmeiser, M. R. *Adv. Synth. Catal.* **2003**, *345*, 996.

(11) See the following for leading references on other types of immobilized catalysts: (a) Nguyen, S. T.; Grubbs, R. H. *J. Organomet. Chem.* **1995**, *497*, 195. (b) Ahmed, M.; Barrett, A. G. M.; Braddock, D. C.; Cramp, S. M.; Procopiou, P. A. *Tetrahedron Lett.* **1999**, *40*, 8657. (c) Audic, N.; Clavier, H.; Mauduit, M.; Guillemin, J.-C. *J. Am. Chem. Soc.* **2003**, *125*, 9248. (d) Garber, S. B.; Kingsbury, J. S.; Gray, B. L.; Hoveyda, A. H. *J. Am. Chem. Soc.* **2000**, *122*, 8168. (e) Kingsbury, J. S.; Garber, S. B.; Giftos, J. M.; Gray, B. L.; Okamoto, M. M.; Farrer, R. A.; Fourkas, J. T.; Hoveyda, A. H. *Angew. Chem.* **2001**, *113*, 4381; *Angew. Chem., Int. Ed.* **2001**, *40*, 4251. (f) Yao, Q. *Angew. Chem.* **2000**, *112*, 4060; *Angew. Chem., Int. Ed.* **2000**, *39*, 3896. (g) Jafarpour, L.; Heck, M.-P.; Baylon, C.; Lee, H. M.; Mioskowski, C.; Nolan, S. P. *Organometallics* **2002**, *21*, 671. (h) Dowden, J.; Savovic, J. *Chem. Commun.* **2001**, 37. (i) Wijkens, P.; Jastrzebski, J. T. B. H.; van der Schaaf, P. A.; Kolly, R.; Hafner, A.; van Koten, G. *Org. Lett.* **2000**, *2*, 1621. (j) Randl, S.; Buschmann, N.; Connon, S. J.; Blechert, S. *Synlett* **2001**, 1547. (k) Connon, S. J.; Blechert, S. *Bioorg. Med. Chem. Lett.* **2002**, *12*, 1873. (l) Connon, S. J.; Dunne, A. M.; Blechert, S. *Angew. Chem.* **2002**, *114*, 3989; *Angew. Chem., Int. Ed.* **2002**, *41*, 3835. (m) Melis, K.; de Vos, D.; Jacobs, P.; Verpoort, F. *J. Mol. Catal. A: Chem.* **2001**, *169*, 47. (n) Akiyama, R.; Kobayashi, S. *Angew. Chem.* **2002**, *114*, 2714; *Angew. Chem., Int. Ed.* **2002**, *41*, 2602. (o) Grela, K.; Tryznowski, M.; Bieniek, M. *Tetrahedron Lett.* **2002**, *43*, 9055. (p) Varray, S.; Lazaro, R.; Martinez, J.; Lamaty, F. *Organometallics* **2003**, *22*, 2426.

(12) For Pd-NHC complexes with hydroxyalkyl side chains and their immobilization see: Schwarz, J.; Böhm, V. P. W.; Gardiner, M. G.; Grosche, M.; Herrmann, W. A.; Hieringer, W.; Raudaschl-Sieber, G. *Chem. Eur. J.* **2000**, *6*, 1773.

Scheme 1^a

^a Conditions: [a] 6-bromo-1-hexanol, THF, reflux, 34% (**5a**); or 3-bromopropanol, THF, reflux, 28% (**5b**); or 4-bromo-2-methyl-2-butanol, toluene, reflux, 65% (**5c**); or 2-bromoethanol, toluene, reflux, 83% (**5d**); [b] (Me₃Si)₂NH, Me₃SiCl cat., CH₂Cl₂, reflux, quant.; [c] complex **1**, KOTBu, toluene, rt, 40% (**7a**), 26% (**7b**), 38% (**7c**), 25% (**7d**); [d] ethereal HCl cat., CH₂Cl₂/MeOH, quant.

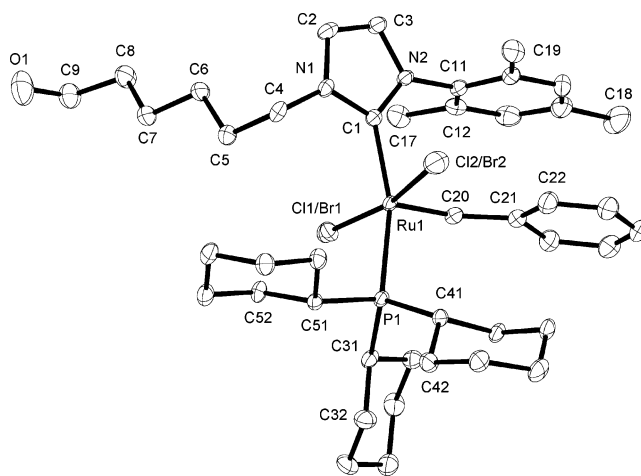


Figure 1. Molecular structure of complex **8a** in the solid state. Hydrogen atoms have been omitted for clarity. Thermal ellipsoids are drawn at 50% probability.

crystal structure analysis for complexes **8a** and **8b** (Figures 1 and 2).

The molecular geometry of **8a** and **8b** is close to square pyramidal as previously observed for compounds of this type^{7,13,14} with P1–Ru–C1 angles of 161° and 162° and Cl–Ru–Cl angles of 168° and 166°, respectively. In **8b** the planarity of these four ligands has an rms of 0.03 Å and the ruthenium atom is positioned 0.32 Å above this plane.¹⁵ The phenyl ring of the apical benzylidene ligand and the *N*-mesityl substituent of the NHC are almost coplanar, with ring distances of 3.21 Å and tilt angles of only 7.7° for **8a** and 10.4° for **8b**.¹⁶ In addition to this π - π interaction, which was previously recognized as a conserved structural characteristic

(13) Fürstner, A.; Thiel, O. R.; Lehmann, C. W. *Organometallics* **2002**, *21*, 331–335.

(14) Love, J. A.; Sanford, M. S.; Day, M. W.; Grubbs, R. H. *J. Am. Chem. Soc.* **2003**, *125*, 10103.

(15) These values are similar to those reported for an asymmetrically substituted NHC with a *tert*-butyldimethylsilyloxyethyl group on one of its *N*-substituents, cf. ref 7.

(16) Determined as described in: Gould, R. O.; Gray, A. M.; Taylor, P.; Walkinshaw, M. D. *J. Am. Chem. Soc.* **1985**, *107*, 5921.

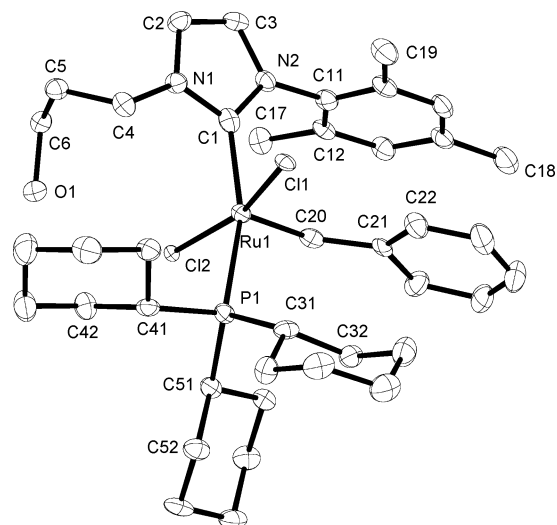
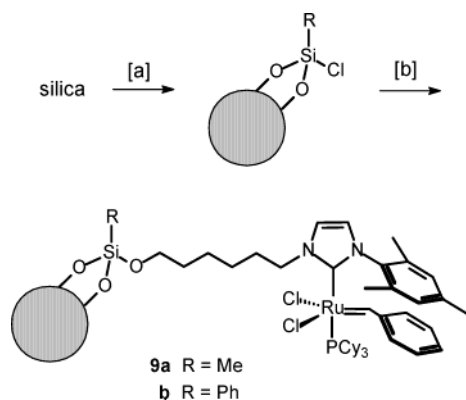


Figure 2. Molecular structure of complex **8b** in the solid state. Hydrogen atoms have been omitted for clarity. Thermal ellipsoids are drawn at 50% probability.

Scheme 2^a



^a Conditions: [a] PhSiCl₃ or MeSiCl₃, CH₂Cl₂, ambient temperature, 30 min; [b] complex **8a**, CH₂Cl₂, 5 min.

of “second-generation” ruthenium carbene complexes,⁷ an O–H···Cl contact of 2.32 Å is found in **8b**. This distance and the H···Cl–Ru angle of 109.1° agree with the averages previously found by Aullón et al.¹⁷ No such contact is found for the hydroxyhexyl derivative **8a**, which exhibits only a long contact toward a dichloromethane solvent molecule.

Complex **8a** can be covalently immobilized on silica, which offers considerable advantages over other support materials due to its low cost, thermal stability, broad solvent compatibility, minimal swelling, and ease of handling. For this purpose, commercial silica gel is treated with RSiCl₃ (R = Me, Ph) in CH₂Cl₂ for 30 min to install stable chlorosilane functionalities on its surface, which serve as appropriate anchor groups for the catalyst (Scheme 2).¹⁸ When complex **8a** is added to a suspension of this material in the same solvent, the solution rapidly becomes colorless, whereas the silica turns dark red-violet, indicating the deposition of the catalyst on the surface. Washing with CH₂Cl₂ does not remove the complex from the support to any noticeable

Table 1. Selected Bond Lengths (Å) and Angles (deg) for Complex **8a**

Ru(1)–C(20)	1.834(4)	C(1)–Ru(1)–Cl(2)	85.79(16)
Ru(1)–C(1)	2.074(4)	C(1)–Ru(1)–Cl(1)	88.4(3)
Ru(1)–P(1)	2.4289(11)	C(20)–Ru(1)–P(1)	99.12(13)
Ru(1)–Cl(1)	2.4230(18)	Cl(2)–Ru(1)–P(1)	90.80(12)
Ru(1)–Cl(2)	2.4033(15)	C(20)–Ru(1)–Cl(2)	102.65(17)
Ru(1)–Br(1)	2.5294(17)	C(20)–Ru(1)–Cl(1)	89.1(3)
Ru(1)–Br(2)	2.5121(19)	Cl(2)–Ru(1)–Cl(1)	167.6(3)
C(20)–C(21)	1.469(6)	C(1)–Ru(1)–P(1)	161.66(11)
N(1)–C(1)	1.359(5)	Cl(1)–Ru(1)–P(1)	91.3(3)
N(2)–C(1)	1.366(5)	N(1)–C(1)–N(2)	103.7(3)
C(20)–Ru(1)–C(1)	99.21(17)	C(21)–C(20)–Ru(1)	137.8(3)

Table 2. Selected Bond Lengths (Å) and Angles (deg) for Complex **8b**

Ru(1)–C(20)	1.825(6)	C(1)–Ru(1)–Cl(1)	86.39(16)
Ru(1)–C(1)	2.052(6)	C(20)–Ru(1)–P(1)	98.52(18)
Ru(1)–P(1)	2.4142(16)	Cl(2)–Ru(1)–P(1)	90.20(5)
Ru(1)–Cl(1)	2.4134(15)	C(20)–Ru(1)–Cl(2)	88.2(2)
Ru(1)–Cl(2)	2.4273(14)	C(20)–Ru(1)–Cl(1)	105.5(2)
C(20)–C(21)	1.472(8)	Cl(2)–Ru(1)–Cl(1)	166.07(5)
N(1)–C(1)	1.362(8)	C(1)–Ru(1)–P(1)	162.18(17)
N(2)–C(1)	1.369(7)	Cl(1)–Ru(1)–P(1)	90.29(5)
C(20)–Ru(1)–C(1)	99.2(2)	N(1)–C(1)–N(2)	103.3(5)
C(1)–Ru(1)–Cl(2)	88.90(16)	C(21)–C(20)–Ru(1)	136.3(5)

Table 3. RCM Reactions Catalyzed by the Immobilized Complex **9a** and Comparison with the Results Obtained Using the Homogeneously Soluble Silyl Ethers **7a,b** (all reactions were carried out with 5 mol % of the active ruthenium component in refluxing CH₂Cl₂ for 24 h; E = COEt)

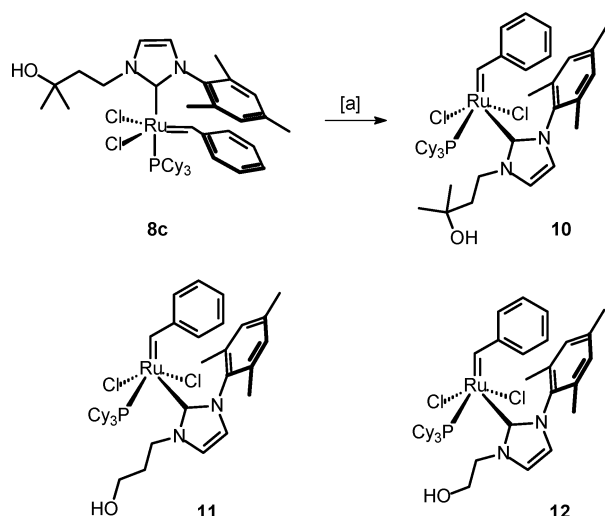
Entry	Product	Yield	
		9a	7
1		98%	95% ^a
2		95%	89% ^a
3		64%	69% ^b
4		75%	
5		81%	81% ^b

^a Using catalyst **7b**. ^b Using catalyst **7a**.

extent; after filtration and drying in vacuo, the functionalized silica gel **9** thus formed is catalytically competent, as shown by the prototype RCM experiments depicted in Table 3. Although longer reaction times are necessary to reach complete conversion, the yields are comparable to those obtained with catalysts **7a,b**, which constitute homogeneously soluble analogues of **9**. After the supported catalyst is filtered off and the solvent is evaporated, the crude products are colorless,¹⁹ thus indicating that the ruthenium species are efficiently retained on the support material, which can be reused up to three times.

(17) Aullón, G.; Bellamy, D.; Brammer, L.; Bruton, E. A.; Orpen, A. G. *Chem. Commun.* **1998**, 653.

(18) Pfleiderer, B.; Albert, K.; Bayer, E. *J. Chromatogr.* **1990**, 506, 343.

Scheme 3^a

^a Conditions: [a] (i) silica gel, CH₂Cl₂; (ii) elution with MeOH, 88%.

In an attempt to immobilize the hydroxyalkyl-functionalized ruthenium carbene complexes by physisorption rather than chemisorption, an unusual molecular rearrangement was observed (Scheme 3). Thus, stirring of a solution of **8c** in the presence of ordinary silica gel leads to an instantaneous color change of the solution from dark red to bright green and the concomitant deposition of the resulting product on the support material. However, the new complex **10** can be eluted from the silica using MeOH as the solvent. Its spectral and analytical data indicate that a rearrangement of the ligand sphere must have taken place. Particularly diagnostic is the benzyldiene proton, which shifts from $\delta_{\text{H}} = 19.57$ (s) in **8c** to $\delta_{\text{H}} = 16.43$ ppm in **10** and splits into a characteristic doublet ($^4J_{\text{P,H}} = 18.7$ Hz); similar changes are observed in the ¹³C and ³¹P NMR spectra (see Experimental Section). The unaltered elemental analysis together with the fact that the free -OH is still clearly visible in the IR spectrum of **10** shows that no intramolecular substitution of one of the chloride ligands by the tethered hydroxyl function has occurred.²⁰ The crystal structure analysis of **10** depicted in Figure 3 confirmed that this sapphire-green complex is isomeric to **8c**, bearing the neutral ligands in a *cis*-rather than the usual *trans* orientation, which is a characteristic and highly conserved structural feature of the Grubbs-type ruthenium carbene complexes known to date.

Complex **10** crystallizes with two independent molecules. The ruthenium center is still found in a nearly square pyramidal geometry with the two chlorine, the phosphine, and the NHC carbon atoms lying in a plane with 0.05 and 0.07 Å rms deviation. As clearly visible from Figure 3, however, the phosphine ligand and the NHC are *cis* rather than *trans* to one another. The

(19) In an experiment using 5 mol % of the immobilized ruthenium complex, analyses (flame ionization detection) show a ruthenium content of only ~250 ppm in the crude product prior to flash chromatography. Thus, ca. 99% of the ruthenium initially used is removed by simple filtration.

(20) (a) It has recently been shown that tethered phenols are able to undergo such intramolecular substitution reactions, cf.: van Veldhuizen, J. J.; Garber, S. B.; Kingsbury, J. S.; Hoveyda, A. H. *J. Am. Chem. Soc.* **2002**, *124*, 4954. (b) See also: Coalter, J. N.; Huffman, J. C.; Caulton, K. G. *Chem. Commun.* **2001**, 1158.

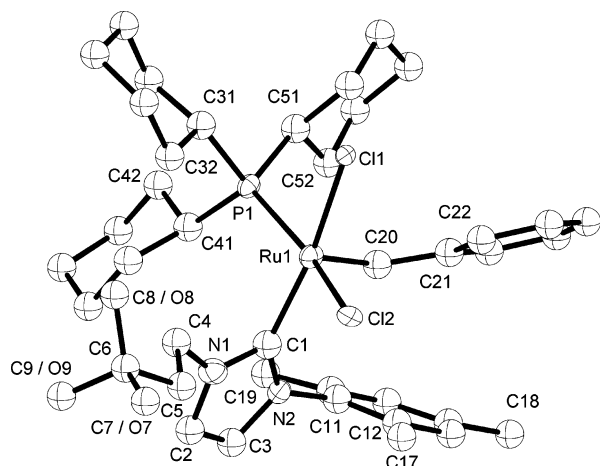


Figure 3. Molecular structure of complex **10** in the solid state. Hydrogen atoms have been omitted for clarity. Thermal ellipsoids are drawn at 50% probability.

Table 4. Selected Bond Lengths (Å) and Angles (deg) for Complex **10**

Ru(1)–C(20)	1.845(7)	C(1)–Ru(1)–Cl(1)	165.0(2)
Ru(1)–C(1)	2.057(8)	C(20)–Ru(1)–P(1)	90.4(2)
Ru(1)–P(1)	2.3520(18)	Cl(2)–Ru(1)–P(1)	161.59(7)
Ru(1)–Cl(1)	2.4444(16)	C(20)–Ru(1)–Cl(2)	107.6(2)
Ru(1)–Cl(2)	2.4507(16)	C(20)–Ru(1)–Cl(1)	102.6(2)
C(20)–C(21)	1.457(10)	Cl(2)–Ru(1)–Cl(1)	84.74(6)
N(1)–C(1)	1.365(10)	C(1)–Ru(1)–P(1)	96.05(19)
N(2)–C(1)	1.392(10)	Cl(1)–Ru(1)–P(1)	87.63(6)
C(20)–Ru(1)–C(1)	91.9(3)	N(1)–C(1)–N(2)	102.6(6)
C(1)–Ru(1)–Cl(2)	87.4(2)	C(21)–C(20)–Ru(1)	127.7(6)

benzyldiene ring is no longer in close contact to the mesityl ring, and the angle between the least-squares planes through these arenes is 32.1° and 33°, respectively. Comparison of the relevant bond lengths shows a considerably shortened Ru–P distance of 2.352(2) Å in the *cis* complex **10**,²¹ whereas in **8a** and **8b** this bond is 2.4289(11) and 2.4142(16) Å due to the *trans* influence exerted by their NHC ligands opposite the Ru–P bond. The dihedral angles P1–Ru–C20–H20 of –52.2° and –55.2° are consistent with the large $^4J_{\text{P,H}} = 18.7$ Hz coupling constant for the benzyldiene proton observed in the ¹H NMR spectrum, indicating that the structure in solution closely resembles that in the solid state.²²

The hydroxyalkyl-functionalized ruthenium carbene complex **8b** undergoes the same rearrangement to the corresponding *cis*-configured complex **11** on contact with silica.²³ This tendency is even more pronounced for the shorter homologue bearing an N-hydroxyethyl side chain, which upon release from its precursor **7d** by deprotection of the terminal TMS group with ethereal HCl does not afford a stable *trans* product **8d** but instantaneously rearranges to the *cis*-configured complex **12** even in the absence of any additional promoter.

(21) The average ruthenium-phosphorus distance in compounds with a *trans* Cl–Ru–P arrangement, however, is even shorter (2.290 Å), while the corresponding *cis* geometry has an average Ru–P bond length of 2.336 Å. These values are statistical averages obtained by analyzing 189 and 2025 corresponding bond lengths found in the CSD.

(22) Grubbs et al. proposed a Karplus-type relation between the dihedral angle P–Ru–C_α–H_α and the observed coupling constant $J_{\text{P,H}}$, cf.: Dias, E. L.; Nguyen, S. T.; Grubbs, R. H. *J. Am. Chem. Soc.* **1997**, *119*, 3887.

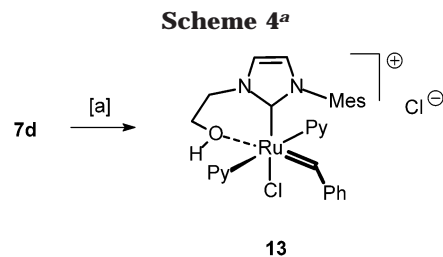
(23) In this context it is noteworthy that attempts to trigger such rearrangements with promoters other than silica were unsuccessful. Specifically, treatment of complex **8b** with ethereal HCl, MgBr₂, AgBF₄, or TMSOTf led to decomposition of the starting complex only.

Surprisingly, the transformation of **7d** into **12** occurs even under mildly basic conditions (Na_2CO_3 in MeOH), although the yield is somewhat lower (70%). Although the mechanism is not yet clear, it is tempting to speculate that the terminal hydroxyl function assists in this reorganization process, which becomes increasingly facile as this group is brought closer to the metal center. This interpretation is in line with the fact that complex **8a** bearing a hydroxyhexyl side chain is the only one that does not rearrange, likely because back-biting of its terminal $-\text{OH}$ would require the transient closure of a kinetically unfavorable 10-membered ring. In any case, the pronounced bias of short-chain hydroxyalkyl-functionalized ruthenium carbene complexes to bring the bulky neutral ligands into a *cis* orientation is in striking contrast to the well-documented structural preferences of virtually all other Grubbs-type catalysts known to date. Only by the use of chelating diphosphines with small bite angles was it possible so far to enforce a *cis*-configured ligand sphere similar to that spontaneously formed in products **10–12**.^{24,25}

Other noteworthy features of these *cis*-configured products are their high polarity and stability. Whereas ruthenium carbene complexes are known to react with primary alcohols, affording catalytically inactive ruthenium carbonyl complexes,²⁶ compounds **10–12** are stable in solution and in the solid state for extended periods of time. However, they exhibit catalytic activity at elevated temperatures, where they likely revert into the red *trans*-form as suggested by pertinent ³¹P NMR data.²⁷

An even more unusual reactivity pattern was found in an attempt to enforce intramolecular nucleophilic displacement of a chloride atom by the (masked) hydroxyl group in the lateral chain to form a chelate structure. Rather than inducing such cyclization, treatment of the silylated complex **7d** with pyridine in CH_2Cl_2 at ambient temperature results in an unprecedented ionization of the complex with formation of the *cationic* ruthenium carbene species **13** (Scheme 4). Its structure in the solid state is depicted in Figure 4.

Compound **13** is six-coordinate with an octahedral ligand sphere. A formal replacement of one chloride and the phosphine by two pyridine ligands has taken place, and the hydroxyethyl side chain now acts as the sixth ligand to the central metal atom. The long distance between ruthenium and oxygen atoms (2.297(7) Å) is inconsistent with a σ -bond but rather indicates a donor–acceptor interaction between these sites, although the



^a Conditions: [a] pyridine, CH_2Cl_2 , rt, 1 h, 82%.

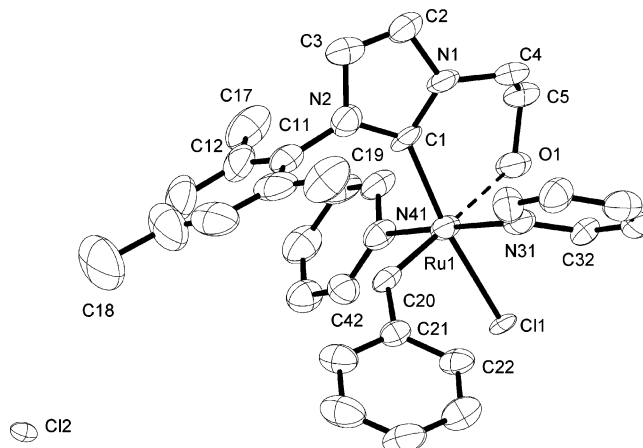


Figure 4. Molecular structure of complex **13** in the solid state. Hydrogen atoms have been omitted for clarity. Thermal ellipsoids are drawn at 50% probability.

Table 5. Selected Bond Lengths (Å) and Angles (deg) for Complex 13

Ru(1)–C(20)	1.866(10)	C(1)–Ru(1)–N(31)	90.0(4)
Ru(1)–C(1)	2.067(10)	C(20)–Ru(1)–N(41)	89.5(4)
Ru(1)–Cl(1)	2.477(2)	C(1)–Ru(1)–N(41)	93.7(4)
C(20)–C(21)	1.465(14)	N(31)–Ru(1)–N(41)	173.4(3)
Ru(1)–N(31)	2.096(9)	C(20)–Ru(1)–O(1)	176.7(4)
Ru(1)–N(41)	2.121(8)	C(1)–Ru(1)–O(1)	85.9(4)
Ru(1)–O(1)	2.297(7)	N(31)–Ru(1)–O(1)	87.6(3)
N(1)–C(1)	1.365(13)	C(1)–Ru(1)–Cl(1)	170.9(3)
N(2)–C(1)	1.348(13)	N(31)–Ru(1)–Cl(1)	90.2(2)
		N(41)–Ru(1)–Cl(1)	85.3(2)
C(20)–Ru(1)–C(1)	94.3(4)	O(1)–Ru(1)–Cl(1)	85.02(18)
C(20)–Ru(1)–N(31)	95.6(4)	N(2)–C(1)–N(1)	105.1(9)

proton on O1 was not found during the course of the crystal structure determination. The octahedral geometry is characterized by the mutual *trans* orientations between the two pyridine ligands as well as the NHC ligand and the remaining chloride. All other structural features are inconspicuous; specifically, the Ru–benzylidene bond length of 1.866(10) Å is not significantly longer than in previously determined structures of the five-coordinate type, and the Ru–NHC bond length of 2.067(10) Å also falls into the established range.^{7,13,14} Both pyridine ligands have the same distance to the metal atom. No π -interaction between the benzylidene and the N-mesityl groups is observed.

Although the proton of the coordinated $-\text{OH}$ group could not be localized in the crystal structure analysis, the strong absorption at $\nu = 3432 \text{ cm}^{-1}$ in the IR spectrum and a broad singlet at $\delta = 9.23 \text{ ppm}$ in the ¹H NMR spectrum unequivocally confirm its presence and thereby corroborate the above structure assignment. The characteristic signals of the benzylidene group ($\delta_{\text{H}} = 18.64 \text{ (s)}$, $\delta_{\text{C}} = 327.6 \text{ ppm}$) in the NMR spectra exclude

(24) (a) Hansen, S. M.; Volland, M. A. O.; Rominger, F.; Eisenträger, F.; Hofmann, P. *Angew. Chem.* **1999**, *111*, 1360; *Angew. Chem., Int. Ed.* **1999**, *38*, 1273. (b) Hansen, S. M.; Rominger, F.; Metz, M.; Hofmann, P. *Chem. Eur. J.* **1999**, *5*, 557. (c) Volland, M. A. O.; Straub, B. F.; Gruber, I.; Rominger, F.; Hofmann, P. *J. Organomet. Chem.* **2001**, *617–618*, 288.

(25) We are aware of only one example in which a ruthenium carbene complex bearing nonchelating ligands crystallizes with its neutral ligands being *cis* disposed. This complex is phosphine free and bears two pentafluorophenoxide moieties instead of the chloride ligands, cf.: Conrad, J. C.; Amoroso, D.; Czechura, P.; Yap, G. P. A.; Fogg, D. E. *Organometallics* **2003**, *22*, 3634.

(26) (a) Dinger, M. B.; *Mol. J. C. Organometallics* **2003**, *22*, 1089. (b) Dinger, M. B.; *Mol. J. C. Eur. J. Inorg. Chem.* **2003**, 2827. (c) Werner, H.; Grünwald, C.; Stürer, W.; Wolf, J. *Organometallics* **2003**, *22*, 1558.

(27) According to ³¹P NMR, stirring of a solution of the *cis* complex **11** in the presence of PCy_3 (1 equiv) in toluene-*d*₈ at 80 °C for 2 h re-converts it into the *trans* analogue **8b**; however, traces of unidentified decomposition products (ca. 10%) are also detected.

that the loss of one chloride has led to the formation of a ruthenium alkylidyne.²⁸

Complex **13** is surprisingly stable even in air and can be recrystallized from EtOH. Although chloride dissociation has previously been shown to increase the catalytic activity of ruthenium carbene complexes to a considerable extent,²⁴ complex **13** is inactive in standard RCM experiments. This is likely due to the pyridine ligands that are tightly bound to the cationic and hence rather Lewis-acidic metal center and cannot be released even upon addition of *p*-TsOH.²⁹ Attempts to enforce cyclization with formation of a covalent O–Ru bond on treatment of **13** with various nonnucleophilic bases were unsuccessful, resulting in the decomposition of the complex only. Although these results have not led to more active metathesis catalysts yet, they highlight several previously unknown facets of the chemistry of ruthenium carbene complexes such as their aversion for alkoxide ligands³⁰ and an as yet unexplored fluxionality of the ligand sphere. Further studies aiming at a better understanding of these properties and the design of catalysts with improved application profiles are underway and will be reported in due course.

Experimental Section

General Considerations. All reactions were carried out under Ar. The solvents were dried by distillation over the following drying agents prior to use and were transferred under Ar: THF, Et₂O (Mg-anthracene), CH₂Cl₂ (P₄O₁₀), toluene (Na). Flash chromatography: Merck silica gel, type 9385, 230–400 mesh. NMR: Spectra were recorded on a Bruker DPX 300, AV 400, or DMX 600 spectrometer; chemical shifts (δ) are given in ppm relative to TMS, coupling constants (*J*) in Hz. MS: Finnigan MAT 8200 (70 eV). ESI-MS: Hewlett-Packard HP 5989 B MS-Engine. HR-MS: Finnigan MAT 95. IR: Nicolet FT-7199 spectrometer. Elemental analyses: H. Kolbe, Mülheim/Ruhr. All commercially available reagents were used as received.

3-(2-Hydroxyethyl)-1-(2,4,6-trimethylphenyl)imidazolium Bromide (5d). A solution of *N*-mesitylimidazole **4** (0.930 g, 5 mmol) and 2-bromoethanol (0.625 g, 5 mmol) in toluene (15 mL) is refluxed for 18 h. For workup, the mixture is diluted with methyl *tert*-butyl ether and washed with water (2 × 15 mL), the aqueous layer is extracted twice with *tert*-butyl ether, the solvent is evaporated, and the residue is triturated with CH₂Cl₂. The CH₂Cl₂ extract is dried over Na₂SO₄ and evaporated to give product **5d** as a pale brown solid (1.29 g, 83%). ¹H NMR (CD₂Cl₂, 300 MHz): δ 9.67 (s, 1H), 8.04 (s, 1H), 7.26 (s, 1H), 7.03 (s, 2H), 5.00–4.85 (br, 1H), 4.73 (t, 2H, *J* = 4.7 Hz), 3.96 (t, 2H, *J* = 4.7 Hz), 2.33 (s, 3H), 2.06 (s, 3H). ¹³C NMR (CD₂Cl₂, 75 MHz): δ 141.2, 137.5, 134.4, 130.7, 129.6, 123.9, 122.9, 59.8, 52.1, 20.8, 17.4. IR (KBr): 3282, 3128, 3059, 2949, 2920, 2872, 1607, 1565, 1546, 1486, 1446, 1206, 1159, 1071, 856, 668 cm⁻¹. MS (ESI): *m/z* 231 [M⁺ – Br]. The

imidazolium salts **5a–c** were prepared analogously. Their analytical and spectral data are compiled below.

3-(6-Hydroxyhexyl)-1-(2,4,6-trimethylphenyl)imidazolium Bromide (5a). The reaction is carried out in THF as the solvent. ¹H NMR (CD₂Cl₂, 300 MHz): δ 10.38 (s, 1H), 7.64 (s, 1H), 7.13 (s, 1H), 6.98 (s, 2H), 4.58 (t, 2H, *J* = 6.8 Hz), 3.48 (t, 2H, *J* = 5.6 Hz), 3.29 (br, 1H), 2.28 (s, 3H), 2.00 (m, 8H), 1.50–1.25 (m, 6H). ¹³C NMR (CD₂Cl₂, 75 MHz): δ 142.1, 139.5, 135.1, 131.6, 130.6, 124.3, 123.6, 62.5, 50.9, 49.8, 32.9, 30.6, 27.5, 26.1, 25.3, 21.7, 18.4. IR (KBr): 3376, 3119, 3061, 2933, 2859, 2743, 1608, 1564, 1546, 1486, 1460, 1411, 1380, 1329, 1289, 1271, 1203, 1162, 1107, 1069, 1039, 968, 935, 856, 760, 731, 672, 639, 579 cm⁻¹. MS (ESI): *m/z* 287 [M⁺ – Br]. Anal. Calcd for C₁₈H₂₇N₂OBr: C, 58.85; H, 7.36. Found: C, 58.85; H, 7.33.

3-(3-Hydroxypropyl)-1-(2,4,6-trimethylphenyl)imidazolium Bromide (5b). The reaction is carried out in THF as the solvent. ¹H NMR (CD₂Cl₂, 300 MHz): δ 10.15 (s, 1H), 7.98 (s, 1H), 7.25 (s, 1H), 7.04 (s, 2H), 4.70 (t, 2H, *J* = 6.2 Hz), 4.80–4.30 (br, 1H), 3.58 (t, 2H, *J* = 5.3 Hz), 2.35 (s, 3H), 2.20–2.00 (m, 2H), 2.08 (s, 6H). ¹³C NMR (CD₂Cl₂, 75 MHz): δ 141.3, 138.1, 134.4, 130.8, 129.7, 123.4, 123.3, 56.9, 47.3, 33.0, 20.8, 17.4. IR (KBr): 3321, 3061, 3010, 2943, 2861, 1562, 1542, 1485, 1208, 1163, 1079, 1066, 1008, 952, 866, 760 cm⁻¹. MS (ESI): *m/z* 245 [M⁺ – Br]. Anal. Calcd for C₁₅H₂₁BrN₂O (325.25): C, 55.39; H, 6.51; N, 8.61. Found: C, 55.19; H, 6.57; N, 8.65.

3-(3-Hydroxy-3-methylbutyl)-1-(2,4,6-trimethylphenyl)imidazolium Bromide (5c). ¹H NMR (DMSO-*d*₆, 400 MHz): δ 9.50 (s, 1H), 8.14 (s, 1H), 7.91 (s, 1H), 7.15 (s, 2H), 4.39 (t, 2H, *J* = 4.7 Hz), 2.33 (s, 3H), 2.02 (m, 8H), 1.18 (s, 6H). ¹³C NMR (DMSO-*d*₆, 100 MHz): δ 140.5, 137.7, 134.7, 131.6, 129.5, 124.0, 123.6, 68.5, 46.4, 42.4, 29.8, 20.9, 17.3. IR: 3361, 3122, 3064, 2970, 2871, 1608, 1565, 1547, 1486, 1460, 1379, 1203, 1162, 1069, 938, 856, 731 cm⁻¹. MS (ESI): *m/z* 273 [M⁺ – Br]. HR-MS calcd 273.1967, found 273.1965. Anal. Calcd for C₁₇H₂₅N₂OBr: C, 57.79; H, 7.08. Found: C, 57.59; H, 7.15.

3-(6-Trimethylsilyloxyhexyl)-1-(2,4,6-trimethylphenyl)imidazolium Bromide (6a). Trimethylchlorosilane (ca. 100 μ L) is added to a solution of imidazolium salt **5a** (602 mg, 2 mmol) in (Me₃Si)₂NH (15 mL) and CH₂Cl₂ (5 mL), and the resulting mixture is refluxed for 24 h. After evaporation of all volatile components, the residue is washed with Et₂O and dried in vacuo to give product **6a** as a pale brown solid (748 mg, quant.). ¹H NMR (CD₂Cl₂, 300 MHz): δ 10.61 (s, 1H), 7.52 (s, 1H), 7.12 (s, 1H), 6.98 (s, 2H), 4.57 (t, 2H, *J* = 7.2 Hz), 3.48 (t, 2H, *J* = 6.2 Hz), 2.28 (s, 3H), 2.02 (s, 6H), 1.91 (m, 2H), 1.42 (m, 2H), 1.33 (m, 4H), 0.03 (s, 9H). ¹³C NMR (CD₂Cl₂, 75 MHz): δ 142.2, 139.6, 135.2, 131.6, 130.6, 123.9, 123.1, 63.0, 51.1, 33.3, 31.2, 27.6, 26.1, 21.7, 18.3, 1.7. IR: 3239, 3111, 3033, 2952, 2861, 2744, 1608, 1564, 1546, 1487, 1475, 1412, 1382, 1329, 1250, 1205, 1181, 1164, 1092, 1070, 1037, 935, 873, 841, 754, 733, 683, 672, 641, 618, 579, 555 cm⁻¹. MS (ESI) *m/z* 345 [M⁺ – Br]. Anal. Calcd for C₂₁H₃₅N₂OSiBr: C, 57.40; H, 7.97. Found: C, 57.24; H, 7.89. The other silylated imidazolium salts were prepared analogously; their spectral and analytical data are compiled below.

3-(3-Trimethylsilyloxypropyl)-1-(2,4,6-trimethylphenyl)imidazolium bromide (6b). ¹H NMR (CD₂Cl₂, 400 MHz): δ 10.42 (s, 1H), 7.55 (s, 1H), 7.05 (s, 1H), 6.93 (s, 2H), 4.62 (t, 2H, *J* = 6.8 Hz), 3.57 (t, 2H, *J* = 5.6 Hz), 2.23 (s, 3H), 2.13 (m, 2H), 1.98 (s, 6H), 0.07 (s, 9H). ¹³C NMR (CD₂Cl₂, 100 MHz): δ 146.6, 142.3, 139.6, 135.3, 131.7, 130.6, 124.2, 123.6, 59.5, 48.6, 34.7, 21.8, 18.4, 1.7. IR: 3123, 3053, 2922, 2868, 2750, 1608, 1565, 1547, 1486, 1455, 1415, 1381, 1331, 1292, 1248, 1206, 1161, 1109, 1069, 969, 934, 898, 855, 841, 751, 671, 580 cm⁻¹. MS (ESI): *m/z* 227 [M⁺ – Br]. Anal. Calcd for C₁₈H₂₉N₂OSiBr: C, 54.41; H, 7.30; Found: C, 54.58; H, 7.37.

3-(3-Trimethylsilyloxy-3-methylbutyl)-1-(2,4,6-trimethylphenyl)imidazolium Bromide (6c). ¹H NMR (DMSO-*d*₆, 300 MHz): δ 9.35 (s, 1H), 8.00 (s, 1H), 7.80 (s, 1H), 7.02 (s,

(28) On treatment with certain aryloxides, ruthenium carbene complexes are prone to loss of one chloride ligand and the benzylidene proton to give the corresponding alkylidyne complexes, cf. ref 25 and the following: (a) Coalter, J. N.; Bollinger, J. C.; Eisenstein, O.; Caulton, K. G. *New J. Chem.* **2000**, *24*, 925. (b) See also: Lynn, D. M.; Grubbs, R. H. *J. Am. Chem. Soc.* **2001**, *123*, 3187.

(29) For a study on the preparation and catalytic activity of neutral pyridine adducts of "second-generation" ruthenium carbene complexes see: Love, J. A.; Morgan, J. P.; Trnka, T. M.; Grubbs, R. H. *Angew. Chem., Int. Ed.* **2002**, *41*, 4035–4037.

(30) The only well-characterized ruthenium carbene complex bearing alkoxide ligands is the formal 14-electron bis-*tert*-butoxide species (tBuO)₂(PCy₃)Ru=CHPh, which is also devoid of catalytic activity in standard metathesis experiments, cf.: Sanford, M. S.; Henling, L. M.; Day, M. W.; Grubbs, R. H. *Angew. Chem.* **2000**, *112*, 3593; *Angew. Chem., Int. Ed.* **2000**, *39*, 3451.

2H), 4.22 (t, 2H, $J = 7.83$ Hz), 2.20 (s, 3H), 1.95 (t, 2H, $J = 7.83$ Hz), 1.89 (s, 6H), 1.16 (s, 6H), 0.01 (s, 9H). ^{13}C NMR (DMSO- d_6 , 75 MHz): δ 140.6, 137.6, 134.6, 131.6, 129.6, 124.1, 123.7, 72.9, 46.3, 43.7, 29.9, 20.9, 17.3, 2.9. IR (KBr) 3132, 3092, 3027, 2975, 1609, 1567, 1547, 1488, 1460, 1383, 1248, 1209, 1154, 1051, 1029, 1018, 874, 841, 760 cm^{-1} . MS (ESI): m/z 345 [$\text{M}^+ - \text{Br}$]. HR-MS calcd 345.2362, found 345.2362. Anal Calcd for $\text{C}_{20}\text{H}_{33}\text{N}_2\text{OSiBr}$: C, 56.47; H, 7.76. Found: C, 56.55; H, 7.71.

3-(2-Trimethylsilyloxyethyl)-1-(2,4,6-trimethylphenyl)imidazolium Bromide (5d). ^1H NMR (CD_2Cl_2 , 300 MHz): δ 10.15 (s, 1H), 7.74 (s, 1H), 7.04 (s, 1H), 6.96 (s, 2H), 4.73 (t, 2H, $J = 4.8$ Hz), 3.94 (t, 2H, $J = 4.8$ Hz), 2.25 (s, 3H), 1.98 (s, 6H), 0.04 (s, 9H). ^{13}C NMR (CD_2Cl_2 , 75 MHz): δ 141.2, 137.5, 135.4, 130.8, 129.6, 124.9, 122.9, 62.5, 53.5, 21.9, 18.5, 0.3. IR (KBr): 3119, 3070, 2958, 1633, 1608, 1565, 1545, 1485, 1445, 1390, 1366, 1249, 1215, 1200, 1163, 1106, 1080, 1062, 941, 843, 760, 752, 669, 614, 576 cm^{-1} . MS (ESI): m/z 223 [$\text{M}^+ - \text{Br}$]. Anal Calcd for $\text{C}_{17}\text{H}_{27}\text{N}_2\text{OSiBr}$: C, 53.26; H, 7.04; N, 7.32. Found: C, 53.03; H, 6.77; N, 7.19.

Complex 7a. KOtBu (112 mg, 1.0 mmol) is added to a solution of the imidazolium salt **6a** (439 mg, 1.0 mmol) and the ruthenium carbene complex **1** (823 mg, 1.0 mmol) in toluene (50 mL), and the resulting mixture is stirred for 1 h at ambient temperature. Evaporation of the solvent followed by flash chromatography of the residue (*n*-pentane/Et₂O, 4:1) affords complex **7a** as a red solid (347 mg, 40%). ^1H NMR (C_6D_6 , 400 MHz): δ 19.68 (s, 1H), 8.30–8.10 (br, 2H), 7.05 (m, 2H), 6.86 (t, 2H, $J = 8.0$ Hz), 6.41 (m, 1H), 6.06 (br, 2H), 4.56 (t, 2H, $J = 6.8$ Hz), 3.42 (t, 2H, $J = 6.8$ Hz), 2.64–2.42 (m, 3H), 2.03 (s, 6H), 1.71 (s, 3H), 1.98–0.90 (m, 38 H), 0.09 (s, 9H). ^{31}P NMR (160 MHz, C_6D_6): δ 34.9. IR (KBr): 3166, 3128, 3098, 3055, 3015, 2926, 2850, 1610, 1588, 1568, 1533, 1490, 1445, 1409, 1383, 1327, 1298, 1248, 1173, 1092, 1028, 1005, 935, 894, 871, 845, 741, 730, 693, 686, 584 cm^{-1} . MS (ESI): m/z 851 [$\text{M}^+ - \text{Cl}$]. Anal Calcd for $\text{C}_{46}\text{H}_{73}\text{N}_2\text{ORuPSiCl}_2$: C, 61.27; H, 8.10. Found: C, 61.16; H, 8.11. Complexes **7b–d** were prepared analogously; their analytical and spectroscopic data are compiled below.

Complex 7b. ^1H NMR (C_6D_6 , 400 MHz): δ 19.64 (s, 1H), 8.12 (m, 2H), 7.02 (m, 3H), 6.85 (t, 1H, $J = 8.0$ Hz), 6.68 (s, 1H), 6.07 (m, 2H), 4.80 (t, 2H, $J = 7.2$ Hz), 3.58 (t, 2H, $J = 6.4$ Hz), 2.56–2.34 (m, 5H), 2.01 (s, 6H), 1.71 (s, 3H), 1.81–1.00 (m, 30H), –0.01 (s, 9H). ^{31}P NMR (C_6D_6 , 160 MHz): δ 35.2. IR (KBr): 3153, 3114, 3063, 3015, 2922, 2848, 1609, 1591, 1490, 1445, 1411, 1386, 1355, 1325, 1291, 1260, 1249, 1234, 1192, 1172, 1098, 1029, 1004, 966, 929, 914, 896, 875, 840, 738, 698, 683, 524 cm^{-1} . MS (ESI): m/z 823 [$\text{M}^+ - \text{Cl}$]. Anal Calcd for $\text{C}_{43}\text{H}_{67}\text{N}_2\text{ORuPSiCl}_2$: C, 60.07; H, 7.80. Found: C, 60.14; H, 7.62.

Complex 7c. ^1H NMR (CD_2Cl_2 , 400 MHz): δ 19.18 (s, 1H), 7.99 (br, 2H), 7.33 (m, 2H), 7.02 (t, 2H, $J = 7.2$ Hz), 6.92 (m, 1H), 6.24 (br, 2H), 4.77 (t, 2H, $J = 6.8$ Hz), 3.14 (br, 1H), 2.28–2.15 (m, 3H), 2.26 (s, 3H), 1.86 (s, 6H), 1.65–1.50 (m, 15H), 1.33 (s, 6H), 1.30–1.00 (m, 15 H), 0.14 (s, 9H). ^{31}P NMR (CD_2Cl_2 , 122 MHz): δ 32.0. IR (KBr): 3171, 3135, 3106, 3059, 2925, 2850, 1488, 1446, 1248, 1173, 1157, 1032, 840, 737, 687 cm^{-1} . MS (ESI): m/z 852 [$\text{M}^+ - \text{Cl}$]. Anal Calcd for $\text{C}_{45}\text{H}_{71}\text{N}_2\text{ORuPSiCl}_2$: C, 60.88 H, 8.00. Found: C, 60.81; H, 8.11.

Complex 7d. ^1H NMR (CD_2Cl_2 , 400 MHz): δ 19.20 (s, 1H), 7.86 (br, 2H), 7.50–7.25 (m, 2H), 7.12 (t, 2H, $J = 7.8$ Hz), 6.80 (m, 1H), 6.30 (m, 2H), 4.83 (t, 2H, $J = 4.7$ Hz), 4.35 (t, 2H, $J = 4.7$ Hz), 2.45–2.05 (m, 3H), 2.34 (s, 3H), 1.92 (s, 6H), 1.90–1.50 (m, 15H), 1.45–1.05 (m, 15H), 0.09 (s, 9H). ^{31}P NMR (CD_2Cl_2 , 122 MHz): 35.6. IR (KBr): 3167, 3130, 3098, 3056, 2925, 2850, 1609, 1569, 1489, 1445, 1409, 1382, 1299, 1261, 1250, 1232, 1200, 1174, 928, 881, 846, 738, 730, 694, 685, 582 cm^{-1} . MS (ESI): m/z 809 [$\text{M}^+ - \text{Cl}$]. Anal Calcd for $\text{C}_{42}\text{H}_{65}\text{N}_2\text{ORuPSiCl}_2$: C, 59.64; H, 7.69. Found: C, 59.88; H, 7.74.

Benzylidene(dichloro-(3-(6-hydroxyhexyl)-1-(2,4,6-trimethylphenyl)imidazolin-2-ylidene)(tricyclohexylphos-

phine)ruthenium (8a). Saturated ethereal HCl (ca. 100 μL) is added to a solution of complex **7a** (225 mg, 0.025 mmol) in CH_2Cl_2 (10 mL) and MeOH (10 mL), and the resulting mixture is stirred for 5 min. The solvent is evaporated to give complex **8a** as a red solid material, which can be recrystallized from $\text{CH}_2\text{Cl}_2/n$ -pentane (207 mg, quant.). ^1H NMR (400 MHz, CD_2Cl_2): δ 19.22 (s, 1H), 8.10–7.70 (br, 2H), 7.39 (t, 1H, $J = 7.2$ Hz), 7.25 (s, 1H), 7.10 (t, 2H, $J = 8.0$ Hz), 6.82 (m, 1H), 6.28 (br, 2H), 4.68 (t, 2H, $J = 8.0$ Hz), 3.69 (t, 2H, $J = 6.8$ Hz), 3.39 (s, 1H), 2.45–2.00 (m, 7H), 2.31 (s, 3H), 1.91 (s, 6H), 1.90–1.86 (m, 3H), 1.68–1.54 (m, 25H), 1.38–1.00 (m, 18H). ^{31}P NMR (160 MHz, CD_2Cl_2): δ 34.4. IR (KBr): 3461, 3163, 3127, 3100, 3059, 2925, 2851, 1610, 1569, 1490, 1445, 1408, 1355, 1325, 1289, 1263, 1238, 1174, 1129, 1072, 1034, 935, 915, 895, 848, 815, 736, 696, 686, 643, 582, 512 cm^{-1} . MS (ESI): m/z 795 [$\text{M}^+ - \text{Cl}$]. UV-vis (CH_2Cl_2): λ_{max} 505 nm. Anal Calcd for $\text{C}_{43}\text{H}_{65}\text{N}_2\text{ORuPCl}_2$: C, 62.24; H, 7.84. Found: C, 62.25; H, 7.78. Complexes **8b** and **8c** were prepared analogously; their spectroscopic and analytical data are compiled below.

Complex 8b. ^1H NMR (400 MHz, CD_2Cl_2): δ 18.98 (s, 1H), 7.90–7.60 (br, 2H), 7.35 (t, 1H, $J = 8.0$ Hz), 7.21 (s, 1H), 7.05 (t, 2H, $J = 8.0$ Hz), 6.82 (d, 1H, $J = 2.4$ Hz), 6.30–6.10 (br, 2H), 5.22 (br, 1H), 4.68 (br, 2H), 3.58 (m, 2H), 2.30–2.20 (m, 8H), 1.86 (s, 6H), 1.85–1.00 (m, 30H). ^{31}P NMR (160 MHz, CD_2Cl_2): δ 36.0. IR (KBr): 3396, 3164, 3125, 3098, 3059, 3022, 2925, 2849, 1708, 1608, 1589, 1568, 1547, 1489, 1446, 1409, 1383, 1350, 1334, 1299, 1231, 1200, 1173, 1072, 968, 950, 934, 897, 847, 739, 696, 686, 585. MS (ESI): m/z 753 [$\text{M}^+ - \text{Cl}$]. UV-vis (CH_2Cl_2): λ_{max} 505 nm. Anal Calcd for $\text{C}_{40}\text{H}_{57}\text{N}_2\text{ORuPCl}_2$: C, 60.99; H, 7.24. Found: C, 61.08; H, 7.34.

Complex 8c. ^1H NMR (C_6D_6 , 400 MHz): δ 19.57 (s, 1H), 8.05 (br, 2H), 7.04 (br, 1H), 6.85 (m, 3H), 6.50 (m, 1H), 6.07 (m, 2H), 4.74 (m, 2H), 2.60–1.00 (m, 51H). ^{31}P NMR (162 MHz): δ 34.7. IR (KBr): 3171, 3135, 3106, 3059, 2925, 2854, 1485, 1447, 1404, 1375, 1229, 1174, 1129, 930, 850, 736, 726 cm^{-1} . MS (ESI): m/z 779 [$\text{M}^+ - \text{Cl}$], 743 [779 – HCl]. UV-vis (CH_2Cl_2): λ_{max} 505 nm. Anal Calcd for $\text{C}_{42}\text{H}_{63}\text{N}_2\text{ORuPCl}_2$: C, 61.84; H, 7.73. Found: C, 61.88; H, 7.62.

Benzylidene-(cis)-dichloro-(3-(3-hydroxy-3,3-dimethylpropyl)-1-(2,4,6-trimethylphenyl)imidazolin-2-ylidene)(tricyclohexylphosphine)ruthenium (10). Silica gel (ca. 5 g) is added to a solution of complex **8c** (408 mg, 0.5 mmol) in CH_2Cl_2 (25 mL), and the resulting suspension is vigorously stirred for 1 min. The dark green silica is filtered off and is carefully washed with CH_2Cl_2 (15 mL) until the filtrate is colorless. The green complex is then eluted from the support using MeOH (25 mL) as the solvent, the filtrate is evaporated, and the residue is recrystallized from $\text{CH}_2\text{Cl}_2/n$ -pentane (8:1) to give product **10** as a green solid (359 mg, 88%). Single crystals suitable for X-ray analysis were grown by diffusing *n*-pentane into a solution of **10** in acetone. ^1H NMR (CD_2Cl_2 , 600 MHz): δ 16.43 (d, 1H, $J = 18.7$ Hz), 7.83 (br, 2H), 7.57 (t, 1H, $J = 7.6$ Hz), 7.28 (m, 2H), 7.20 (d, 1H, $J = 2.0$ Hz), 6.98 (s, 1H), 6.73 (d, 1H, $J = 2.0$ Hz), 6.17 (s, 1H), 5.25–5.36 (m, 1H), 4.37 (m, 1H), 2.44 (m, 1H), 2.42 (s, 3H), 2.21 (m, 3H), 2.19 (s, 3H), 2.02 (m, 1H); 1.96 (br, 3H), 1.85 (br, 3H), 1.75 (br, 3H), 1.69 (br, 3H), 1.63 (br, 3H) 1.42 (br, 3H), 1.37 (s, 3H), 1.32 (s, 3H), 1.31 (s, 3H), 1.30 (s, 3H), 1.17–1.08 (m, 9H). ^{31}P NMR (CD_2Cl_2 , 122 MHz): δ 43.2. ^{13}C NMR (CD_2Cl_2 , 151 MHz): δ 305.0 (d, $J_{\text{PC}} = 16$ Hz), 181.0 (d, $J_{\text{PC}} = 11$ Hz), 149.1 (d, $J_{\text{PC}} = 2$ Hz), 139.3, 139.0, 136.3, 134.4, 130.9, 130.4, 129.0, 127.8, 125.8, 120.9, 69.7, 49.1, 43.1, 31.2, 30.5, 29.6, 28.9, 28.2 (t, $J_{\text{PC}} = 10$ Hz), 27.8 (t, $J_{\text{PC}} = 10$ Hz), 26.8, 20.9, 20.1, 19.0. IR (Nujol): 3435, 3182, 3151, 1609, 1579, 1567, 1261, 1226, 1171, 1073, 1005, 892, 848, 685 cm^{-1} . MS (ESI): m/z 744 [$\text{M}^+ - 2\text{Cl}$]. UV-vis (CH_2Cl_2): λ_{max} 600 nm. Anal Calcd for $\text{C}_{42}\text{H}_{63}\text{N}_2\text{ORuPCl}_2$: C, 61.84; H, 7.73; Cl, 8.71. Found: C, 61.98; H, 7.65; Cl, 8.81.

Complex 11. **11** was prepared as described above using complex **8b** (394 mg, 0.5 mmol) as the starting material. A green solid (334 mg, 85%) was produced. ^1H NMR (CD_2Cl_2 ,

400 MHz): δ 16.31 (d, 1H, $J = 18.8$ Hz), 7.73 (br, 2H), 7.48 (t, 1H, $J = 7.2$ Hz), 7.20 (m, 3H), 6.88 (s, 1H), 6.68 (d, 1H, $J = 2.4$ Hz), 6.07 (s, 1H), 5.17 (dt, 1H, $J = 13.6$ Hz, $J = 8.0$ Hz), 4.39 (m, 1H), 3.63 (m, 2H), 2.65 (br, 1H), 2.35 (s, 3H), 2.15 (m, 2H), 2.08 (s, 3H), 1.90–0.80 (m, 36H). ^{31}P NMR (CD_2Cl_2 , 122 MHz): δ 44.6. IR (KBr): 3436, 3178, 3107, 3055, 3016, 2928, 2851, 1484, 1447, 1402, 1376, 1234, 1173, 1071, 1006, 849, 739, 686 cm^{-1} . MS (ESI): m/z 751 [$\text{M}^+ - \text{Cl}$]. UV–vis (CH_2Cl_2): λ_{max} 600 nm. Anal Calcd for $\text{C}_{40}\text{H}_{57}\text{N}_2\text{ORuPCL}_2$: C, 60.99; H, 7.24. Found: C, 61.15; H, 7.32.

Complex 12. Saturated ethereal HCl (ca. 100 μL) is added to a solution of complex **7d** (85 mg, 0.11 mmol) in $\text{CH}_2\text{Cl}_2/\text{MeOH}$ (1:1, 5 mL). After stirring for 5 min at ambient temperature, all volatile components are evaporated to give product **12** as a green solid (77 mg, quant.). ^1H NMR (CD_2Cl_2 , 400 MHz): δ 17.05 (d, 1H, $J = 17.6$ Hz), 7.95 (d, 2H, $J = 7.2$ Hz), 7.56 (t, 1H, $J = 8.0$ Hz), 7.27 (m, 3H), 6.96 (s, 1H), 6.73 (s, 1H), 6.20 (br, 1H), 4.30 (m, 4H), 3.76 (m, 1H), 2.42 (s, 3H), 2.39–2.19 (m, 3H), 2.17 (s, 6H), 2.05–1.04 (m, 30H). ^{31}P NMR (CD_2Cl_2 , 162 MHz): δ 39.9. IR (KBr): 3178, 3059, 2928, 2849, 1607, 1575, 1484, 1446, 1375, 1328, 1244, 1235, 876, 849, 739, 683 cm^{-1} . MS (ESI): m/z 704 [$\text{M}^+ - 2\text{Cl}$], UV–vis (CH_2Cl_2 , 5 mmol/L): 600 nm. Anal Calcd for $\text{C}_{39}\text{H}_{57}\text{N}_2\text{ORuPCL}_2$: C, 60.54; H, 7.37. Found: C, 60.48; H, 7.18.

Complex 13. A solution of complex **12** (167 mg, 0.2 mmol) in CH_2Cl_2 (5 mL) and pyridine (1 mL) is stirred for 1 h at ambient temperature. The volume is reduced to ca. 2 mL before pentane (10 mL) is carefully added, and the resulting mixture is allowed to stand at ambient temperature for 2 days. The precipitated green complex **13** is filtered off and dried in vacuo (106 mg, 82%). Single crystals suitable for X-ray analysis were grown by diffusing *tert*-butyl methyl ether into a solution of this material in EtOH. ^1H NMR (400 MHz, CD_2Cl_2): δ 18.64 (s, 1H), 9.23 (br, 1H, OH), 8.23 (d, 4H, $J = 5.6$ Hz), 7.63–7.49 (m, 5H), 7.23 (d, 1H, $J = 2.0$ Hz), 7.10 (t, 2H, $J = 7.6$ Hz), 7.05 (t, 4H, $J = 7.6$ Hz), 6.92 (s, 2H), 6.79 (s, 1H), 4.62 (t, 2H, $J = 4.8$ Hz), 3.25 (t, 2H, $J = 4.8$ Hz), 2.39 (s, 3H), 1.34 (s, 6H). ^{13}C NMR (100 MHz, CD_2Cl_2): δ 327.6, 179.4, 155.6, 151.8, 149.0, 139.3, 136.0, 135.2, 135.1, 130.7, 129.8, 128.7, 127.9, 124.2, 124.2, 123.8, 122.9, 60.1, 51.1, 20.2, 16.5. IR (KBr): 3432, 2962, 2925, 2869, 1603, 1586, 1483, 1446, 1404, 1337, 1259, 1098, 1067, 863, 804, 763, 697 cm^{-1} . MS (ESI): m/z 615 [$\text{M}^+ - \text{Cl}$], 536 [$\text{M}^+ - \text{Cl} - \text{py}$], 500 [$\text{M}^+ - 2\text{Cl} - \text{py}$], 421 [$\text{M}^+ - 2\text{Cl} - 2\text{py}$]. Anal Calcd for $\text{C}_{31}\text{H}_{34}\text{N}_4\text{ORuCl}_2$: C, 57.06; H, 5.21. Found: C, 56.89; H, 5.18.

X-ray Crystal Structure Analyses. Data were collected on a Nonius KappaCCD diffractometer at 100 K. Structures were solved by Patterson method (**8b**) or direct methods and refined by full-matrix least-squares using Chebyshev weights on F_o^2 . The hydrogen atoms were included isotropically using a riding model.

Crystal Data for Complex 8a: $\text{C}_{44}\text{H}_{67}\text{Br}_{0.50}\text{Cl}_{3.50}\text{N}_2\text{OPRu}$, $M_w = 936.07$, red needle, crystal size $0.13 \times 0.09 \times 0.03$ mm, triclinic, $P\bar{1}$ [No. 2], $a = 9.69720(10)$ Å, $b = 12.5345(2)$ Å, $c = 18.5673(3)$ Å, $\alpha = 80.4820(10)^\circ$, $\beta = 85.4340(10)^\circ$, $\gamma = 81.6710(10)^\circ$, $V = 2198.72(5)$ Å³, $Z = 2$, $D_x = 1.414$ g cm^{-3} , $\lambda = 0.71073$ Å, $\mu(\text{Mo K}\alpha) = 1.095$ mm⁻¹, $3.49^\circ < \theta < 31.17^\circ$, psi-scan absorption correction, 43301 measured, 13 744 independent reflections, 9880 with $I > 2\sigma(I)$. $R_1 = 0.067$ [$I > 2\sigma(I)$], $wR_2 = 0.159$, 502 parameters, $S = 1.08$, residual electron density $+1.6/-1.7$ e Å⁻³, CCDC 215571.

Crystal Data for Complex 8b: $\text{C}_{41.50}\text{H}_{62}\text{Cl}_5\text{N}_2\text{OPRu}$, $M_w = 914.22$, red plate, crystal size $0.22 \times 0.19 \times 0.12$ mm, monoclinic, $P2_1/n$ [No. 14], $a = 17.3808(9)$ Å, $b = 12.0539(7)$ Å, $c = 22.7446(12)$ Å, $\beta = 106.951(2)^\circ$, $V = 4558.1(4)$ Å³, $Z = 4$, $D_x = 1.332$ g cm^{-3} , $\lambda = 0.71073$ Å, $\mu(\text{Mo K}\alpha) = 0.704$ mm⁻¹, $1.74^\circ < \theta < 23.27^\circ$, Gaussian absorption correction ($T_{\text{max}} = 0.92$, $T_{\text{min}} = 0.86$), 30 188 measured, 6527 independent reflections, 4498 with $I > 2\sigma(I)$. $R_1 = 0.051$ [$I > 2\sigma(I)$], $wR_2 = 0.141$, 482 parameters, $S = 1.06$, residual electron density $+1.2/-0.7$ e Å⁻³, CCDC 215572.

Crystal Data for Complex 10: $\text{C}_{42.75}\text{H}_{65.50}\text{Cl}_2\text{N}_2\text{O}_{1.25}\text{PRu}$, $M_w = 830.41$, pale green plate, crystal size $0.14 \times 0.12 \times 0.04$ mm, monoclinic, $P2_1/c$ [No. 14], $a = 9.58710(10)$ Å, $b = 23.6782(2)$ Å, $c = 37.7484(4)$ Å, $\beta = 92.23(10)^\circ$, $V = 8562.60(15)$ Å³, $Z = 8$, $D_x = 1.288$ g cm^{-3} , $\lambda = 0.71073$ Å, $\mu(\text{Mo K}\alpha) = 0.562$ mm⁻¹, $3.74^\circ < \theta < 26.79^\circ$, psi-scan absorption correction, 36 272 measured, 14 072 independent reflections, 9594 with $I > 2\sigma(I)$. $R_1 = 0.077$ [$I > 2\sigma(I)$], $wR_2 = 0.217$, 889 parameters, $S = 1.03$, residual electron density $+1.7/-1.1$ e Å⁻³, CCDC 215570.

Crystal Data for Complex 13: $\text{C}_{36}\text{H}_{37}\text{Cl}_2\text{N}_4\text{O}_{3.50}\text{Ru}$, $M_w = 753.67$, blue-violet block, crystal size $0.17 \times 0.15 \times 0.07$ mm, orthorhombic, $Pbca$ [No. 61], $a = 16.1863(3)$ Å, $b = 14.7148(2)$ Å, $c = 31.8092(5)$ Å, $V = 7576.3(2)$ Å³, $Z = 8$, $D_x = 1.321$ g cm^{-3} , $\lambda = 0.71073$ Å, $\mu(\text{Mo K}\alpha) = 0.594$ mm⁻¹, $4.21^\circ < \theta < 23.26^\circ$, psi-scan absorption correction, 16 723 measured, 5210 independent reflections, 3750 with $I > 2\sigma(I)$. $R_1 = 0.087$ [$I > 2\sigma(I)$], $wR_2 = 0.245$, 436 parameters, $S = 1.07$, residual electron density $+1.7/-1.0$ e Å⁻³, CCDC 217824.

Acknowledgment. Generous financial support by the Deutsche Forschungsgemeinschaft (Leibniz award to A.F.) and the Fonds der Chemischen Industrie is gratefully acknowledged.

Supporting Information Available: Complete list of atom coordinates and anisotropic displacement parameters as well as tables containing all bond lengths and bond angles. This material is available free of charge via the Internet at <http://pubs.acs.org>.

OM0342006